Astron. Astrophys. 339, 858–871 (1998)

ASTRONOMY AND ASTROPHYSICS

Towards a fundamental calibration of stellar parameters of A, F, G, K dwarfs and giants*

G.P. Di Benedetto

CNR-Istituto di Fisica Cosmica, Via Bassini 15, I-20133 Milano, Italy (pdibene@ifctr.mi.cnr.it)

Received 25 May 1998 / Accepted 21 August 1998

Abstract. I report on the implementation of the empirical surface brightness technique using the near-infrared Johnson broadband $(V-K)$ colour as suitable sampling observable aimed at providing accurate effective temperatures of 537 dwarfs and giants of A-F-G-K spectral-type selected for a flux calibration of the Infrared Space Observatory (ISO). The surface brightness-colour correlation is carefully calibrated using a set of high-precision angular diameters measured by modern interferometry techniques. The stellar sizes predicted by this correlation are then combined with the bolometric flux measurements available for a subset of 327 ISO standard stars in order to determine one-dimensional $(T, V-K)$ temperature scales of dwarfs and giants. The resulting very tight relationships show an intrinsic scatter induced by observational photometry and bolometric flux measurements well below the target accuracy of $\pm$ 1 % required for temperature determinations of the ISO standards. Major improvements related to the actual direct calibration are the high-precision broadband K magnitudes obtained for this purpose and the use of Hipparcos parallaxes for dereddening photometric data.

The temperature scale of F-G-K dwarfs shows the smallest random errors closely consistent with those affecting the observational photometry alone, indicating a negligible contribution from the component due to the bolometric flux measurements despite the wide range in metallicity for these stars. A more detailed analysis using a subset of selected dwarfs with large metallicity gradients strongly supports the actual bolometric fluxes as being practically unaffected by the metallicity of field stars, in contrast with recent results claiming somewhat significant effects. The temperature scale of F-G-K giants is affected by random errors much larger than those of dwarfs, indicating that most of the relevant component of the scatter comes from the bolometric flux measurements. Since the giants have small metallicities, only gravity effects become likely responsible for the increased level of scatter.

The empirical stellar temperatures with small model-dependent corrections are compared with the semiempirical data by the Infrared Flux Method (IRFM) using the large sample of 327 comparison stars. One major achievement is that all empirical and semiempirical temperature estimates of F-G-K giants and dwarfs are found to be closely consistent between each other to within $\pm$ 1 %. However, there is also evidence for somewhat significant differential effects. These include an average systematic shift of (2.33 ± 0.13) % affecting the A-type stars, the semiempirical estimates being too low by this amount, and an additional component of scatter as significant as $\pm$ 1 % affecting all the comparison stars. The systematic effect confirms the results from other investigations and indicates that previous discrepancies in applying the IRFM to A-type stars are not yet removed by using new LTE line-blanketed model atmospheres along with the updated absolute flux calibration, whereas the additional random component is found to disappear in a broadband version of the IRFM using an infrared reference flux derived from wide rather than narrow band photometric data.

Key words: stars: atmospheres – stars: fundamental parameters

1. Introduction

The fundamental calibration of stellar parameters of solar neighborhood stars provides the most relevant empirical support to many galactic and extragalactic investigations. These include: calibrations of the HR diagram; tests of stellar evolutionary tracks; interpretation of stellar spectra; calibrations of cosmological distance indicators. For instance, the recent developments of infrared astronomy and the new observational windows opened by the Infrared Space Observatory (ISO) for wavelengths up to at least 50 μm has put stringent requirements on the accuracy of the effective temperatures, i.e. as good as $\pm$ 1 %, for detailed interpretations of calibrating stellar spectra related to a large number of solar neighborhood stars (van der Bliek et al. 1992). Then, it becomes of major concern to have reliable methods to determine high-precision stellar temperatures required for this purpose.

Send offprint requests to: G. P. Di Benedetto

Tables 1 and 2 are only/also available in electronic form at the CDS via anonymous ftp to cdsarc.u-strasbg.fr (130.79.128.5) or via http://cdsweb.u-strasbg.fr/Abstract.html

* Table 1 and 2 are only available in the electronic form of this paper

In this paper I shall be concerned with a direct approach in attempting to approximate as much as possible fundamental stellar parameters. The method suggested so far applies the empirical surface brightness technique (Wesselink 1969; Barnes et al. 1978) along with the bolometric flux measurements and relates all the derived stellar parameters to the broadband $(V-K)$ colour as the most suitable and practically unbiased sampling observable (Di Benedetto 1993). The required photometric correlations are carefully calibrated by accurate angular diameters from modern interferometry techniques and by bolometeric flux measurements placed on an updated absolute scale. The spectral range is now extended to cover the field of A-F-G-K dwarf and giant stars. The high-precision near-infrared *K* magnitudes available for this purpose and the Hipparcos parallaxes applied for dereddening photometric data of distant stars have notably provided the most relevant observational support to improve significantly the accuracy of final results.

2. The database

A homogeneous set of 769 photometric standard stars for the ISO mission have been selected as suitable preliminary candidates with spectral types and visual magnitudes derived according to the Hipparcos Input Catalogue (Turon et al. 1992). High-precision broadband *K* magnitudes have been measured for 565 stars of the Northern Hemisphere in the TCS magnitude system (Hammersley, to be published) and for 204 stars of the Southern Hemisphere in the ESO magnitude system (van der Bliek, Bouchet & Manfroid 1996) with 35 stars in common. All the near-infrared data have been converted into the Johnson magnitude system, i.e. the standard reference photometry of the calibrations throughout this paper, according to the following transformations:

$$\begin{aligned}(V-K_{\rm TCS}) &= 0.057 + 0.985(V-K)\\ &\quad [\Delta(V-K) = 0.039\,mag; N = 64\,Stars]\\ (V-K_{\rm ESO}) &= 0.037 + 0.992(V-K)\\ &\quad [\Delta(V-K) = 0.036\,mag; N = 57\,Stars]\end{aligned} \qquad (1)$$

where $\Delta(V-K)$ is the standard error determined from the overall scatter around the mean relation. Since the TCS and ESO near-infrared colours have accuracies of about $\pm$ 0.02 mag, most of the scatter $\Delta(V-K)$ is likely due to the less accurate Johnson near-infrared photometry. The transformations are plotted in Fig. 1.

Most of the 769 stars have their accurate trigonometric parallaxes measured by the Hipparcos satellite (ESA 1997). This provides a valuable step towards a fundamental calibration, since the interstellar extinction to get intrinsic integrated fluxes and colour indices has been derived according to the absolute distances from parallaxes. To be consistent with the bolometric flux measurements, I shall adopt below a visual absorption $A_{\rm V}$ = 0.8 mag/kpc along the line of sight to each star (Blackwell et al. 1990). The near-infrared colour excesses will be derived according to $E_{\rm V-K} = A_{\rm V}$ / 1.1 (Wegner 1994).

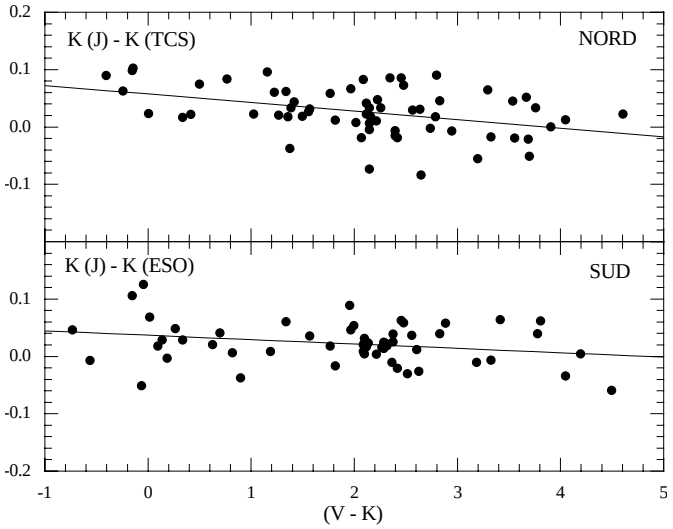

Fig. 1. Comparison between broadband *K* magnitudes against the broadband near-infrared colour on the Johnson scale. Top: Johnson and TCS systems. Bottom: Johnson and ESO systems. Solid lines: least squares fits [see Eqs. (1)]

Several conditions have to be met by the ISO standard stars, if their effective temperatures must be determined at the required target accuracy of $\pm$ 1 %. For this reason, 94 stars have been excluded from the actual calibration, since they are of O, B, M spectral-type and/or of luminosity class I. In addition, a subset of 127 objects is discarded because of their variability in the visible (more than 0.1 mag) or multiplicity according to the Hipparcos Input Catalogue or the absence of Hipparcos data. A further small number of 11 stars have their intrinsic colours out of the overall range $-0.1 \leq (V-K)_{\rm O} \leq 3.7$ covered by the actual calibration of A-F-G-K dwarfs and giants.

The final selected set of 537 stars includes 393 stars observed in the Northern Hemisphere and 144 stars observed in the Southern one with 25 stars in common. The bolometric fluxes along with the broadband near-infrared photometry are only available for a subset of 327 stars with 22 of these having K-magnitudes in both TCS and ESO systems. The bolometric flux measurements have been determined by Blackwell & Lynas-Gray (1998; hereinafter BL) for application of the semiempirical narrowband IRFM to the ISO standard stars. Tables 1 and 2 list the 393 Northern and 144 Southern stars, respectively, with HIC and BS identifications, spectral-type, observational *V, K* photometry, Hipparcos parallax π and bolometric flux $F_{\rm BOL}$. The last two columns report the intrinsic broadband near-infrared colour converted into the Johnson magnitude system according to the Eqs. (1) and the final stellar effective temperature according to the calibrations discussed below.

3. Photometric calibration of stellar parameters

3.1. Photometric calibration of surface brightness scales

The surface brightness of a star of intrinsic magnitude $m_{\rm o}$ and angular diameter ϕ is defined by:

$$S_{\rm M} = m_{\rm o} + 5\log\phi \qquad (2)$$

where the zero-point is chosen such that $S_{\rm M} = m_{\rm o}$ mag when $\phi = 1$ mas. The surface brightness is currently calibrated by measuring the stellar angular diameters of non variable stars. Only recently, late-type stars with apparent angular sizes larger than few milliarcsec have become suitable targets for the modern developed Michelson interferometry techniques. Therefore, many reliable measurements of stellar diameters have become available with uncertainties better than 5 % (Davis & Tango 1986; Di Benedetto & Rabbia 1987; Mozurkewich et al. 1991). Since photometric stellar diameters have to be predicted at the target accuracy better than 2 % for the ISO standards, the currently available surface brightness-colour (SC) correlations should be carefully revisited in order to investigate their sensitivity to different sources of errors. Table 3 lists the sample of angular diameters which will be adopted throughout this paper for the calibration of the SC correlations. Most of these measurements related to giants cooler than the Sun have been already discussed and self-consistent comparisons showed remarkable agreement of independent visual and IR data to less than 2 % of accuracy (Di Benedetto 1993).

Now, the selected sample call for several improvements:

1. The angular diameter of the K-giant Arcturus (α Boo) is available with its well determined limb darkening (Quirrenbach et al. 1996) which was found to be in excellent agreement with the predictions from limb-darkening coefficients for a grid of model atmospheres tabulated by Manduca (1979). This grid has been currently adopted to convert measured uniform disk diameters at visual and infrared wavelengths into true photospheric stellar sizes.
2. The angular diameters of the F dwarf Procyon (α CMi) and the G0 III component of Capella (α Aur) are available from Michelson interferometry with accuracy good enough for including these spectral types into the actual revisited SC correlations.
3. The sample of A-type stars basically relies on the less accurate intensity interferometry data. But it notably includes the most relevant angular size of the star Sirius (α CMa) which has been also measured by Michelson interferometry and the two independent measurements show excellent agreement between each other.
4. Most of the calibrating stars are included in the overall sample of the ISO standards, notably the stars Vega (α Lyr) and Sirius. Sirius has been recently adopted as primary calibrator of the absolute stellar fluxes in the infrared (Cohen et al. 1992). A comparison between the broadband *K* magnitude of Vega in the TCS system and that of Sirius in both TCS and ESO systems shows a somewhat discrepancy with the broadband *K* magnitudes reported by Cohen et al.. Then, to be consistent with this absolute flux calibration, a Johnson near-infrared colour $(V-K) = 0.005$ mag is adopted below for Vega rather than the value of $-$ 0.025 mag determined from the TCS observations.

The visual surface-brightness data are plotted in Fig. 2 as a function of several standard broadband colours in the Johnson magnitude system. Reddening corrections are not applied to the data, since they would induce overall effects on the residuals much smaller than 0.1 mag, all the stars being within 100 pc. As it can be seen, the $(S_{\rm V}, V-K)$ correlation is found to be affected by the smallest scatter. All the other plots show a larger dispersion which is a clear signature that the corresponding standard colours are poorer brightness indicators for the actual high-precision set of angular diameters. Most of this scatter is certainly due to photometric errors and could be likely reduced by using suitable high-precision photometry. However, there is also evidence from theoretical model atmospheres (Bell & Gustafsson 1989, hereinafter BG; Kurucz 1991) that some magnitude-colour combinations notably using optical colours may be biased by gravity and metallicity which would prevent the corresponding photometry to be adopted as a bias-free indicator of stellar sizes.

Fig. 3 shows that a tight $(S_{\rm V}, V-K)$ correlation is found for either the dwarfs which include calibrators of A-F-G spectral-type or the giants which include only stars of G-K spectral-type or both. Then, in applying the near-infrared correlation below, I shall refer to stellar luminosities of Class V and Class III with suitable calibrations given by:

$$
\begin{aligned}
& -0.1 \leq (V-K)_{\rm O} \leq 1.5 \\
S_{\rm V} &= 2.556 + 1.580(V-K)_{\rm O} - 0.106(V-K)^2_{\rm O} \\
& [\Delta S_{\rm V} = 0.03\ mag; N = 9\ Class\ V\ Stars] \\
& 1.5 \leq (V-K)_{\rm O} \leq 3.7 \\
S_{\rm V} &= 2.657 + 1.421(V-K)_{\rm O} - 0.033(V-K)^2_{\rm O} \\
& [\Delta S_{\rm V} = 0.03\ mag; N = 14\ Class\ III\ Stars] \\
& -0.1 \leq (V-K)_{\rm O} \leq 3.7 \\
S_{\rm V} &= 2.563 + 1.493(V-K)_{\rm O} - 0.046(V-K)^2_{\rm O} \\
& [\Delta S_{\rm V} = 0.03\ mag; N = 23\ Class\ V, III\ Stars]
\end{aligned}
\qquad (3)
$$

where $\Delta S_{\rm V}$ is the standard error determined from the overall scatter around the mean relation. The intrinsic colour-index is referred to the Johnson broadband magnitude system. Notice that few data with deviations greater than about 3 $\Delta S_{\rm V}$ are omitted from the final calibration (see Table 3). There would be evidence for a small luminosity effect in the actual calibration of the stellar surface brightness. In fact, around the colour $(V-K) = 1.5$ mag, the Class V and Class III correlations yield the angular diameter of the Sun in error by about + 0.7 % and + 2.0 %, respectively. The result from the Class III correlation would deviate by 1.5 sigma from the average ridge-line. However, in view of the relatively small number of stars involved in the calibration, this luminosity effect should not be overemphasized.

The residual scatter $\Delta S_{\rm V} = 0.03$ mag around the best fitting regression lines is due to random errors in the observed colours and angular diameter measurements. By assuming that there are no errors in the colours, it would lead to an overall uncertainty $\Delta\phi/\phi$ = 1.4 % for angular sizes predicted by observational photometry. If the colours are fitted to surface-brightness data, assuming all of the error in the colours, it would correspond to an error $\Delta(V-K) = 0.02$ mag, quite consistent with the expected uncertainty in the near-infrared photometry of the ISO

Table 3. Nearby stars with accurate measurements of angular diameters

Star		BS	Sp. Type	V	(V-K)	π (mas)	φ ± Δφ (mas)		$(V-K)_O$	S_V (mag)	
α	CMa	2491	A1 V	-1.440	-0.083	378	5.92	0.09 [a]	-0.099	2.419	
				-1.440	-0.111	378					
α	Lyr	7001	A0 V	0.033	0.005	131	3.24	0.07 [b]	-0.001	2.580	
γ	Gem	2421	A0 IV	1.928	0.051	32	1.39	0.09 [b]	0.028	2.618	
ε	Sgr	6879	A0 V	1.836	0.081	21	1.44	0.06 [b]	0.047	2.590	
β	Car	3685	A1 IV	1.672	0.132	29	1.59	0.07 [b]	0.107	2.652	*
β	Leo	4534	A3 V	2.14	0.15	82	1.33	0.10 [b]	0.14	2.750	
α	Psa	8728	A3 V	1.166	0.150	130	2.10	0.14 [b]	0.144	2.771	
α	Oph	6556	A5 III	2.080	0.389	70	1.63	0.13 [b]	0.379	3.129	
α	Aql	7557	A7IV-V	0.765	0.524	195	2.98	0.14 [b]	0.520	3.132	*
α	CMi	2943	F5 IV-V	0.37	1.01	292	5.51	0.05 [c]	1.01	4.073	
	Sun		G2 V	-26.762	1.486		1919260		1.486	4.654	
α	Aur	1708	G0 III	0.78	1.56	80	6.28	0.43 [d]	1.55	4.760	
				0.78	1.56	80	6.42	0.28 [e]	1.55	4.808	
β	Cap	7776	K0 II - III	3.08	2.17	100	3.18	0.15 [f]	2.16	5.584	
β	Gem	2990	K0 III	1.161	2.253	97	7.90	0.31 [g]	2.246	5.641	
				1.161	2.253	97	8.04	0.08 [c]	2.246	5.679	
ε	Cyg	7949	K0 III	2.500	2.414	45	4.62	0.04 [c]	2.398	5.805	*
α	Cas	0168	K0 III	2.23	2.48	16	5.64	0.05 [c]	2.43	5.936	
α	Ari	0617	K2 III	2.00	2.64	49	6.85	0.06 [c]	2.63	6.162	
δ	And	0165	K3 III	3.270	2.876	32	4.12	0.04 [c]	2.853	6.320	*
γ	And	0603	K3 II	2.10	2.91	13	7.50	0.36 [g]	2.85	6.414	
				2.10	2.91	13	7.84	0.07 [c]	2.85	6.510	*
α	Boo	5340	K1 III	-0.050	2.929	89	20.95	0.20 [g]	2.921	6.547	
				-0.050	2.929	89	21.00	0.20 [h]	2.921	6.552	
γ	Dra	6705	K5 III	2.231	3.536	22	10.13	0.24 [g]	3.503	7.223	
				2.231	3.536	22	10.20	0.20 [i]	3.503	7.237	
α	Tau	1457	K5 III	0.867	3.719	50	20.88	0.10 [l]	3.704	7.450	
				0.867	3.719	50	20.21	0.30 [g]	3.704	7.379	*
				0.867	3.719	50	21.21	0.21 [c]	3.704	7.484	

[a] From Davis & Tango (1986)
[b] From Code et al. (1976)
[c] From Mozurkewich et al. (1991)
[d] From Di Benedetto & Bonneau (1991)
[e] From Hummel et al. (1994)
[f] From Ridgway et al. (1980)
[g] From Di Benedetto & Rabbia (1987)
[h] From Quirrenbach et al. (1996)
[i] From Hutter et al. (1989)
[l] From Ridgway et al. (1982)
* Data omitted from the fits

standard stars. By combining the relations (2) and (3), the true photospheric stellar angular diameter is given by:

$$5\log\phi(mas) = S_{\rm V} - (V - A_{\rm V}) \quad (4)$$

where $A_{\rm V}$ is the visual absorption derived from the Hipparcos parallaxes. According to a first-order approximation of $S_{\rm V}$ as a function of the colour, the relation (4) can also be rewritten as:

$$5\log\phi(mas) \approx \alpha + \beta(V-K) - (V - A_{\rm V} + \beta E_{\rm V-K})$$
$$\approx \alpha - \beta K + (\beta - 1)V + [1 - (\beta/1.1)]A_{\rm V} \quad (5)$$

where the slope β increases from about 1.2 for K-type stars to 1.5 for A-type stars. The relation (5) emphasizes that the error on the *K* magnitude will critically contribute to the uncertainty $\Delta(V-K)$. In fact, the same photometric error in the magnitude *K* or in the absorption $A_{\rm V}$ would yield as a negligible contribution as 0.5 %. Notice that an absorption $A_{\rm V} = (0.10 \pm 0.02)$ mag together with a reddening coefficient of 0.8 mag/kpc corresponds to a distance of (125 ± 25) pc.

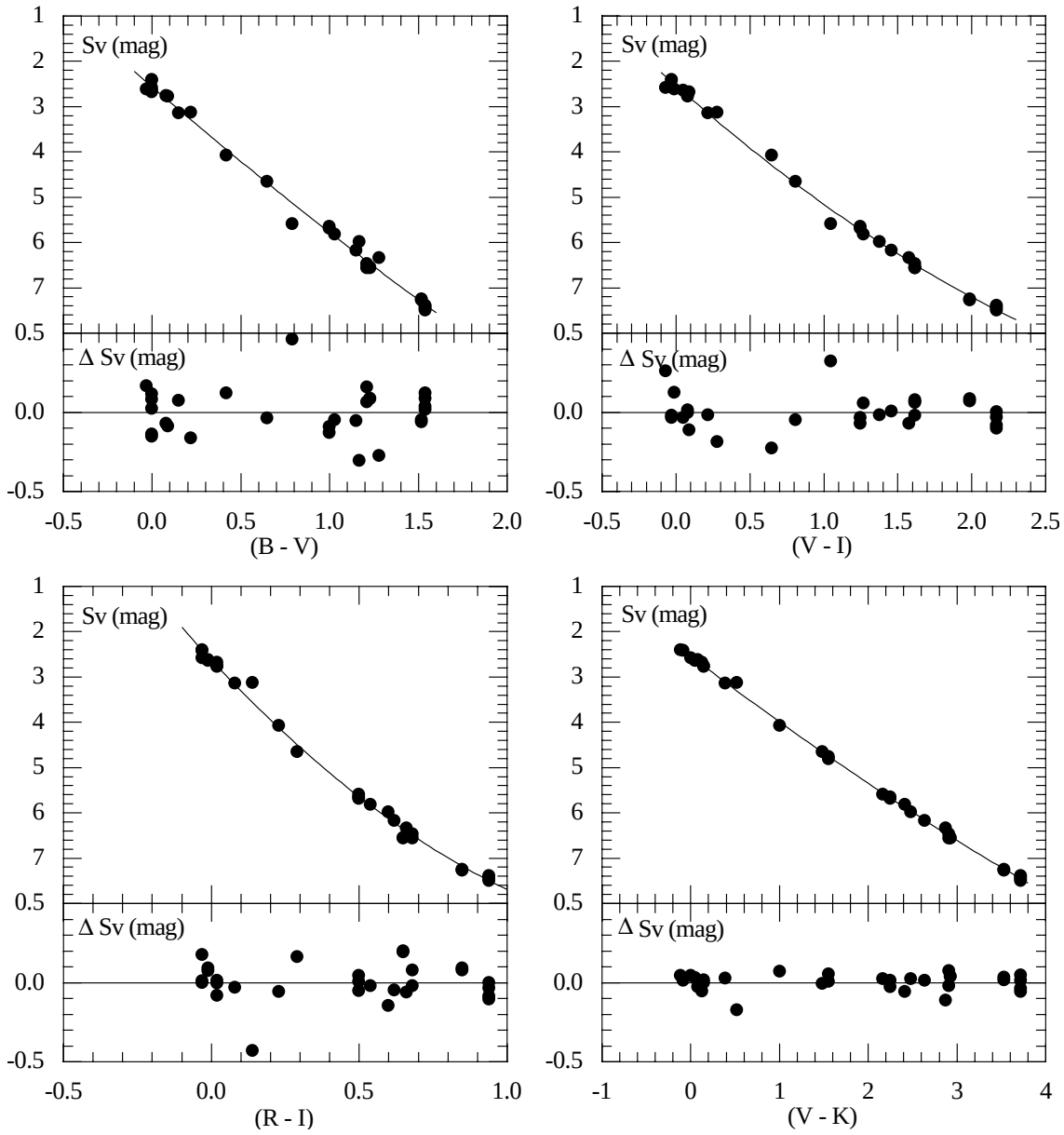

Fig. 2. Visual surface brightness for an angular diameter of 1 mas against several standard broadband colour indices on the Johnson scale. For each diagram, the solid line in the upper panel represents the least-squares quadratic fit to all data with residuals around the ridge-line plotted in the lower panel

There are several potential sources of systematic error which can affect the photometric diameters predictable by the near-infrared $(S_{\rm V}, V-K)$ correlation. First, the correlation strictly refer to either G-K giants or A-F-G dwarfs. To cover the whole A-F-G-K spectral range, the overall correlation must be adopted which fully ignores the small luminosity effects. However, systematic deviations would likely be no more than about 1 %, as shown for the Sun angular diameter. Second, the correlation may suffer from stellar variability, multiplicity, etc. which could induce somewhat significant variations of the visual magnitude *V*. However, these effects are likely to be reduced to a negligible level within the subset of 537 ISO standard stars according to the adopted selection criteria and to the coefficients of the relation (5). Third, the magnitude-colour combination $(V, V-K)$ in the relation (5) is expected to be slightly sensitive to stellar metallicity through line blanketing. This effect can be evaluated by using model-atmosphere results of BG. For a metallicity as poor as $[Fe/H] = -1$ dex, the photometric diameter would change by no more than 1 % with respect to that of metal-normal content over a range of gravities $1.5 < \log g < 4.5$ and effective temperatures $4000 < T < 6500$ K.

It can be concluded that the $(S_{\rm V}, V-K)$ correlation would certainly benefit from a much larger sample of calibrating angular diameters as accurate as 5 % or better for deeper investigating systematic and random errors in the predicted stellar sizes by high-precision near-infrared photometry. However, there seems

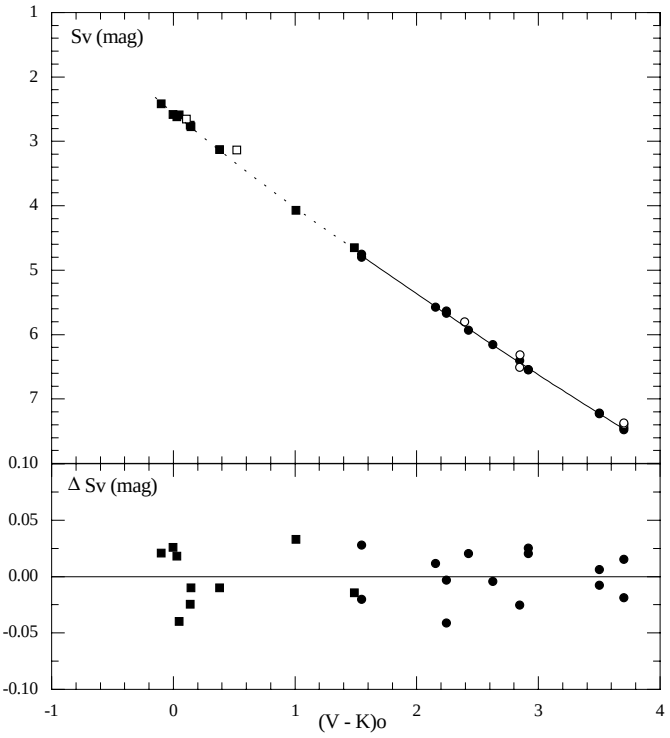

Fig. 3. Calibration of the visual surface brightness for an angular diameter of 1 mas against the intrinsic near-infrared colour. Top: solid and dotted lines represent least squares quadratic fits to data of giants and dwarfs, respectively. Open symbols: data falling more than 3 sigmas away from the lines. Bottom: residuals around each best fitting regression line

to be observational and theoretical evidence that the actual carefully calibrated correlation can likely provide reliable angular diameters with errors smaller than 2 %, implying a target accuracy of less than 1 % for temperature determinations of the ISO standard stars.

3.2. Photometric calibration of bolometric flux parameters

The absolute integrated fluxes of 420 ISO standard stars have been determined by BL for applications of the IRFM. Also, BL widely investigated the several sources of potential errors which can affect flux measurements, and then no further discussion will be done below. I shall adopt throughout this paper these bolometric fluxes for a more straightforward comparison with the IRFM which notably relies on the very recent absolute flux calibration (Cohen et al. 1992). Now, the major concern is related to the bolometric flux representations by the broadband near-infrared colour $(V-K)$ which play a relevant role in the calibration of temperature scales by the actual method. For this purpose, only a subset of 327 stars is available with broadband *K* magnitudes in either the TCS or ESO photometric systems and 22 stars in common. In addition, the bolometric fluxes of 35 giants (Blackwell et al. 1990) have been included in the main list to properly sample the Class III stars of K spectral type. According to BL, these fluxes should be slightly increased by 1.1 % to take into account the change of the absolute calibration. To be consistent with the calibration of the surface brightness scales, the bolometric fluxes are related to the broadband colour $(V-K)$ on the Johnson magnitude system through the convenient flux parameter defined by:

$$\begin{aligned} F_{\rm K} &= -(K_{\rm O} + 2.5\log F_{\rm BOL}) \\ &= (V-K)_{\rm O} - 2.5\log RFLUX \end{aligned} \quad (6)$$

where $F_{\rm BOL}$ is the measured bolometric flux in Wm^{-2} and RFLUX = $F_{\rm BOL}10^{0.4V_{\rm O}}$ is the corresponding "reduced flux" used by BL. The star-by-star values of the parameter $F_{\rm K}$ are plotted in Fig. 4 as a function of the intrinsic colour $(V-K)_{\rm O}$. Regression lines according to standard least-squares quadratic fits have been obtained by assuming accurate intrinsic colour determinations. The regression lines are given by:

$$\begin{aligned} &-0.1 \le (V-K)_{\rm O} \le 0.6 \\ F_{\rm K} &= 18.876 + 1.552(V-K)_{\rm O} - 0.452(V-K)^2_{\rm O} \\ &[\Delta F_{\rm K} = 0.018\ mag; N = 46\ Class\ V\ Stars] \\ &0.7 \le (V-K)_{\rm O} \le 3.0 \\ F_{\rm K} &= 18.986 + 1.134(V-K)_{\rm O} - 0.121(V-K)^2_{\rm O} \\ &[\Delta F_{\rm K} = 0.010\ mag; N = 211\ Class\ V\ Stars] \\ &0.2 \le (V-K)_{\rm O} \le 3.7 \\ F_{\rm K} &= 18.969 + 1.160(V-K)_{\rm O} - 0.124(V-K)^2_{\rm O} \\ &[\Delta F_{\rm K} = 0.024\ mag; N = 137\ Class\ III\ Stars] \end{aligned} \quad (7)$$

where $\Delta F_{\rm K}$ is the standard error determined from the overall scatter around the mean relation. Twenty-one stars have been excluded from the fits (see Tables 1 and 2), since they showed deviations significantly larger than 3 sigmas from the mean fits. The regression line for Class V stars has been obtained over two separate spectral ranges. The advantage is that the residual scatter around the best fitting ridge-line of F-G-K stars is found to be significantly smaller than that of A-type stars. In addition, one can best compare results for Class V and III stars over the same F-G-K spectral range.

The residual scatter $\Delta F_{\rm K}$ about each best-fitting regression line displayied in the lower panels of Fig. 4 is due to random errors in the observed colours and bolometric flux measurements. By assuming that there are no errors in the colours, the scatter yields $\Delta F_{\rm BOL}/F_{\rm BOL} = 1.09\Delta F_{\rm K}$, i.e. 1.1 % and 2.6 % for the integrated fluxes of dwarfs and giants, respectively, over the F-G-K spectral-range. If the colours are fitted to the flux data, assuming all of the error in the colours, the scatter becomes $\Delta(V-K)$ = 0.018 mag for dwarfs, fully consistent with the errors on the near-infrared photometry of the ISO standard stars. But, it would be as large as $\Delta(V-K)$ = 0.049 mag for giants. As the near-infrared broadband colours in either the TCS or ESO magnitude systems have been measured with the same accuracy of $\Delta(V-K) \approx 0.02$ mag regardless of the stellar luminosity class, it follows that the *increased component of scatter* in the

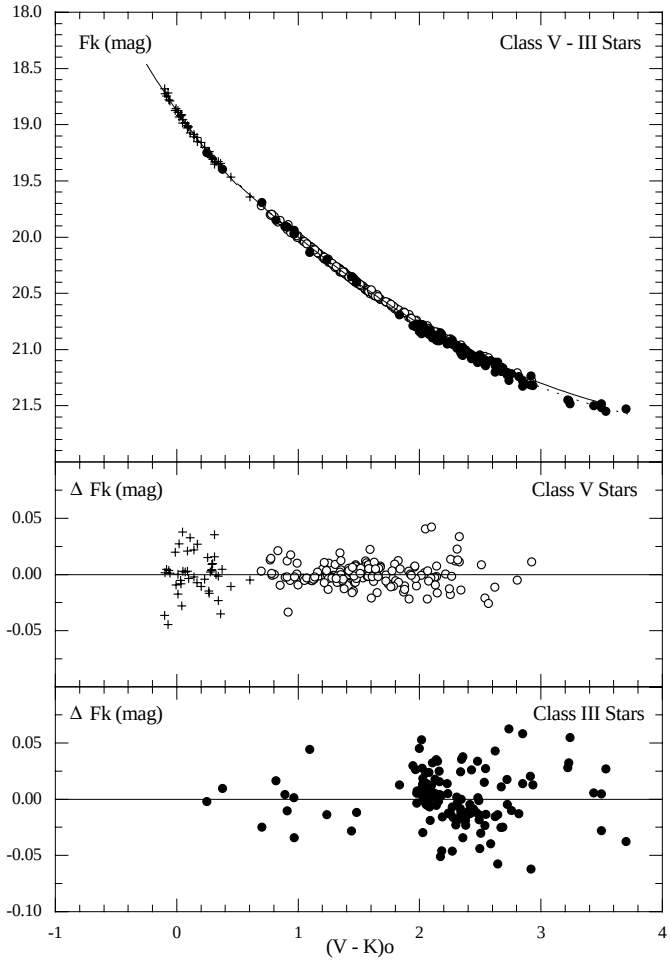

Fig. 4. Calibration of the infrared flux parameter for Class V and III stars against the intrinsic near-infrared colour. Top: plots of individual data with solid and dotted lines representing least-squares quadratic fits to dwarfs and giants, respectively. Middle and bottom: residuals around each best fitting regression line. Crosses indicate A-type stars

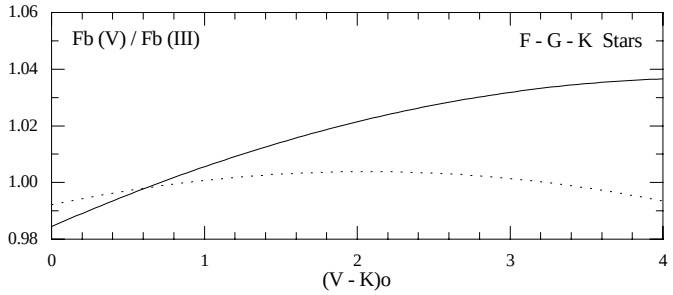

Fig. 5. Solid line: ratio of Class V to Class III bolometric flux representations by second-order polynomials against the intrinsic near-infrared colour. Dotted line: the same ratio with colour shift of one class with respect to other [see text Eq. (8)]

diagram $(F_{\rm K}, V-K)$ of Class III stars must be likely ascribed to the bolometric flux measurements.

The photometric correlations show also evidence for a *real differential effect* between Class III and V stars at the same intrinsic colour. The average difference derived according to the flux representation by the polynomials (7) is drawn in Fig. 5. The figure indicates as well that this effect can be reasonably well compensated for by a colour shift of:

$$(V-K)_{\rm V} = (V-K)_{\rm III} + 0.055 \qquad (8)$$

This shift would enable the Class V and III second-order polynomials (7) to be interchanged for bolometric flux representations of all the F-G-K stars.

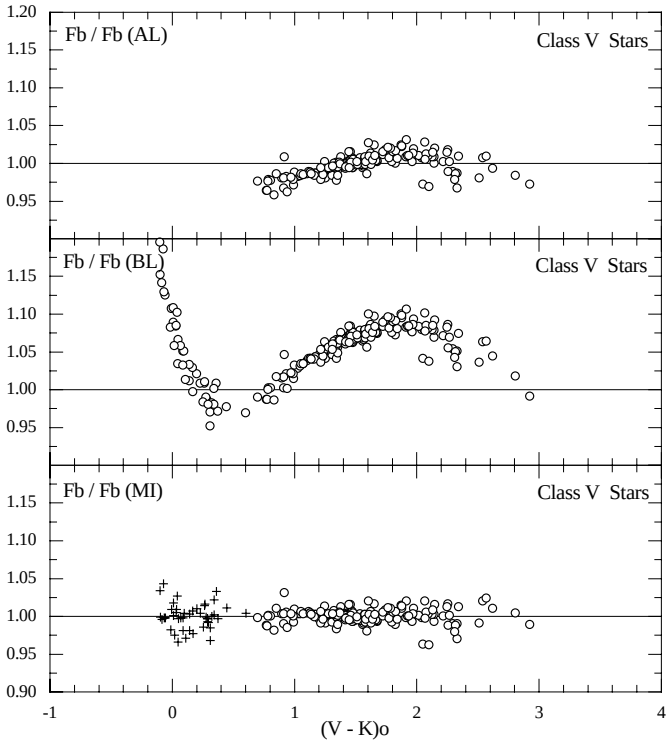

Fig. 6. Comparison of residuals from bolometric flux representations by the broadband near-infrared colour. Top and middle: residuals according to third-order polynomials from Alonso et al. (1995) and BL, respectively. Bottom: residuals according to second-order polynomials with crosses indicate A-type stars

The goodness of the bolometric flux representation by the second-order polynomials (7) can be compared with recent representations by third-order polynomials of the colour $(V-K)$ on the Johnson magnitude scale (Alonso et al. 1995; BL). Fig. 6 shows the bolometric flux residuals for each representation of Class V stars less affected by random errors. The diagrams indicate that a second- order polynomial function suffices to best fit the flux data even at the level of noise as low as that of dwarfs. This improvement may be due either to the use of the flux parameter $F_{\rm K}$ or to the adoption of two separate spectral ranges for regression lines or both.

3.3. Photometric calibration of effective temperature scales

According to the fundamental method, the true photospheric stellar angular diameter ϕ should be combined with the integrated flux $F_{\rm BOL}$, in order to derive the effective temperature

T from the Stefan-Boltzmann law. Then, the temperature determination is given by:

$$\begin{aligned} T(K) &= 1.316 \times 10^6 (F_{\rm BOL}/\phi^2)^{1/4} \\ \log T(K) &= 6.1193 + 0.1[(V-K)_{\rm O} - (F_{\rm K} + S_{\rm V})] \\ &= A + B(V-K)_{\rm O} + C(V-K)^2_{\rm O} \end{aligned} \quad (9)$$

Since both the correlations $S_{\rm V}$ and $F_{\rm K}$ are well-represented by quadratic fits in the colour $(V-K)_{\rm O}$, the calibration of the scale $\log$ T through the coefficients A, B, C immediately follows as a second-order polynomial function of the same colour. Table 4 reports these coefficients suitable over specific colour ranges together with the overall accuracies for predicted temperatures.

These results call for several remarks.

1. The first three colour ranges have both the correlations $S_{\rm V}$ and $F_{\rm K}$ properly sampled by suitable calibrating stars and are selected to maintain as far as possible the peculiarities of the spectral ranges notably the small luminosity effects. According to these effects, a temperature shift of T(V) - T(III) = 57 K would be observed around the colour $(V-K)_{\rm O}$ = 1.5, corresponding to a difference of about 1 % for the Sun temperature mainly due to the contribution from the $S_{\rm V}$ correlation.
2. The next three colour ranges are not properly sampled by calibrating angular diameters and adopt the overall surface-brightness correlation (3) which fully ignores the luminosity effects on the $S_{\rm V}$ data.
3. The colour range 0.7–3.7 for Class V and III stars adopts the overall surface-brightness correlation (3) along with the $F_{\rm K}$ correlation derived by averaging the corresponding correlations of Class V and III stars. Then, it fully ignores luminosity effects on both the $S_{\rm V}$ and $F_{\rm K}$ data. All temperatures of the ISO standards lacking luminosity classification have been derived according to this scale.
4. The overall accuracy Δ T / T quoted in Table 4 takes into account independent sources of error, added quadratically, intrinsic to the calibration. These include a conservative error $\Delta(V-K) = \pm$ 0.02 mag consistent with the lower dispersion observed in the $S_{\rm V}$ and $F_{\rm K}$ data and the errors $\Delta S_{\rm V}$ and $\Delta F_{\rm K}$ from the calibrations themselves. As it can be seen, the required target accuracy of $\pm$ 1 % is achievable for all temperatures of the ISO standards, but not for A-type stars with $(V-K)_{\rm O} \leq 0.6$ mag. For these stars, the observational photometry becomes the dominant source of uncertainty owing to the steeper slope of the temperature scale $(T, V-K)$.

The star-by-star representations of the $(T, V-K)$ scales are plotted in Fig. 7 along with the residuals around the average correlations of Table 4. The scales are as tight as the corresponding $(F_{\rm K}, V-K)$ scales drawn in Fig. 4, since a smoothed $(S_{\rm V}, V-K)$ correlation is applied in any case for deriving temperatures by the relation (9). The relation (9) makes also clear the overall strategy adopted to provide the final effective temperatures as a function of the near-infrared broadband colour for all the 537 ISO standard stars. Accordingly, all individual temperatures appear to be well represented by second-order polynomial functions with the scatter induced by observational photometry and bolometric flux measurements alone. The worse results for Class III stars due to the increased scatter in the bolometric flux measurements are also evident. All the individual temperatures are reported in the last column of Tables 1 and 2.

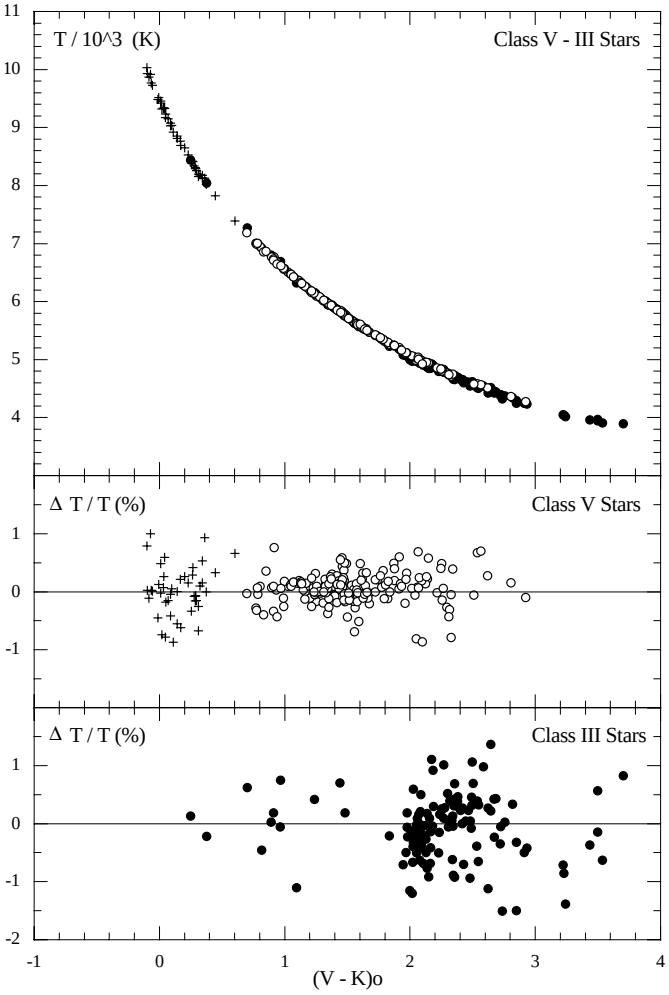

Fig. 7. Top: plots of individual temperatures for Class V and III stars as a function of the intrinsic near-infrared colour. Middle and bottom: residuals from temperature scales represented by the second-order polynomials of Table 4. Crosses indicate A-type stars

The broadband near-infrared temperatures can also be exploited as high-precision calibrating data for assessing random and systematic errors affecting other photometric temperature scales. For instance, the $(T, B-V)$ scale shown in Fig. 8 looks quite different because of the increased errors affecting the optical colour-index. These include systematic effects due to stellar gravity and metallicity biasing the colours of giants and dwarfs. Therefore, the scale must include evaluations of gravity and metallicity of stars in order to get reliable and accurate individual results. Notice that the superimposed systematic effects tend to compensate for the small temperature shift between the luminosity classes observed in the near-infrared diagram $(T, V-K)$.

Table 4. Calibration of $\log T$ scales as a function of the Johnson broadband $(V-K)$ colour

$(V-K)_O$	Luminosity	Spectrum	A	B	C	$\Delta T / T$ (%)
- 0.1 – 0.7	V	A	3.9762	- 0.2110	0.0468	1.2 – 1.0
0.7 – 1.5	V	F - G	3.9651	- 0.1713	0.0227	0.9 – 0.8
1.5 – 3.7	III	G - K	3.9567	- 0.1581	0.0157	0.9 – 0.8
- 0.1 – 0.7	III	A	3.9762	- 0.2110	0.0468	1.2 – 1.0
1.5 – 3.0	V	G - K	3.9644	- 0.1627	0.0166	0.8 – 0.7
0.7 – 1.5	III	F - G	3.9662	- 0.1653	0.0169	1.0 – 0.8
0.7 – 3.7	V - III	F - G - K	3.9653	- 0.1640	0.0168	1.0 – 0.8

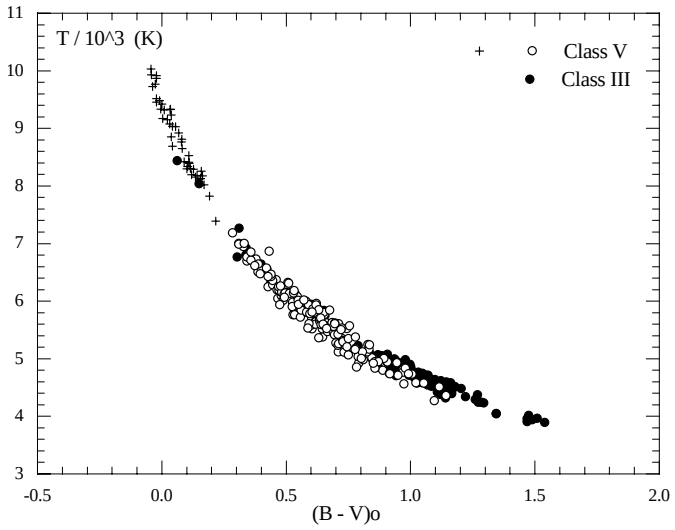

Fig. 8. The same as the top panel of Fig. 7 as a function of the optical colour index

4. Comparison with direct measurements of stellar parameters

The first most obvious step is to compare the photometric estimates of stellar parameters with the direct measurements available for the calibrating stars of Table 3. Table 5 summarizes the results for eight of the most relevant comparison stars. The errors of each indirect determination are omitted, being not of relevance for the present purposes. Indeed, it can be seen that all photometric estimates show a very close agreement with the corresponding direct measurements at less than two sigmas, except for the Vega's flux. Of course, this good agreement is to be expected for angular diameters, all stars being primary calibrators of the $S_{\rm V}$ correlation of Fig. 3. However, this is not the case for the predicted fluxes and then for the final temperatures of these stars. Notably, it should be appreciated the indirect determination of the Sun's temperature according to its well-determined near-infrared colour in the Johnson magnitude system (Campins et al. 1985). There are also somewhat discrepant data which include the angular diameter of α CMi (1.6 SD) and the bolometric fluxes of α Lyr (2.4 SD) and α Boo (1.4 SD). The corresponding photometric temperatures differ by no more than 1 % from the measured ones, except the temperature of α Lyr which shows a discrepancy as large as 2 % mainly due to the difference of about 10 % between predicted and measured bolometric fluxes. In fact, the integrated flux of α Lyr is not correctly represented by its *V, K* photometry, in contrast with its photometric angular size nearly close to the interferometric measurement. Notice that, by using the TCS colour of $(V-K)$ = − 0.025 mag, the photometric diameter would decrease to the value 3.13 mas now discrepant at 1.6 SD with the measured one, but the flux would increase by only 1 % leaving the significant flux discrepancy unsolved.

On the other hand, this flux discrepancy seems to affect only the star α Lyr, as it can be seen from the additional flux data listed in Table 6. Here, all the calibrating A-type stars of Table 3 are reported with their integrated fluxes. For all stars, but not for α Lyr, the agreement is remarkably good at the 4 % level of accuracy quoted for each determination. This comparison enables us to estimate as well the amount of systematic error due to independent absolute calibrations which might affect flux determinations. With the exception of α Lyr, the average difference is found to be as small as $\Delta F_{\rm BOL}/F_{\rm BOL} \approx 0.5$ %. This remarkable consistency for the critical field of A-type stars gives a further valuable support to the reliability of photometric temperatures for the ISO standard stars at the target accuracies quoted in Table 4, but not for α Lyr whose flux discrepancy remains an unsolved problem.

Table 5. Comparison between measured and predicted stellar parameters by broadband photometry

Star	V_O	$(V-K)_O$	ϕ (mas)	F_{BOL} ($\times 10^{-9}$ W m^{-2})	T (K)	ΔT (K)
α CMa			5.92 ± 0.09	114.3 ± 4.4 [a]	9945 ± 122	
	- 1.442	- 0.099	5.86	112.2	9943	- 2
α Lyr			3.24 ± 0.07	30.4 ± 1.2 [a]	9660 ± 140	
	0.027	- 0.001	3.20	27.5	9469	- 191
α CMi			5.51 ± 0.05	18.08 ± 0.76 [a]	6501 ± 74	
	0.37	1.01	5.43	17.93	6538	37
SUN			1.919 10^6	(1375 ± 14)10^9 [b]	5786 ± 40	
	- 26.762	1.486	1.932 10^6	1373 10^9	5763	- 23
β Gem			8.04 ± 0.08	10.97 ± 0.44 [c]	4750 ± 53	
	1.153	2.246	8.05	11.40	4795	45
α Boo			20.97 ± 0.20	49.68 ± 1.99 [d]	4291 ± 48	
	- 0.059	2.921	20.76	46.90	4255	- 36
γ Dra			10.16 ± 0.20	8.49 ± 0.34 [d]	3964 ± 55	
	2.194	3.503	10.17	8.27	3941	- 23
α Tau			21.05 ± 0.20	33.81 ± 1.35 [d]	3890 ± 43	
	0.851	3.704	21.07	32.65	3859	- 31

[a] From Code et al. (1976)
[b] From Forgan (1977)
[c] From Blackwell & Lynas-Gray (1998)
[d] From Blackwell et al. (1990)

5. Comparison with the semiempirical Infrared Flux Method

It is of the utmost importance that as a large number as 327 ISO standard stars have their temperatures well determined by the semiempirical narrowband IRFM and by the actual empirical broadband near-infrared approach, since comparisons between the independent results can be done at the best level of available accuracies. One best compares diameters rather than temperatures, since any detectable difference between the results is enhanced by a factor two and the suitable reference can rely on the observational correlation of Fig. 3 independent of absolute flux calibrations. Fig. 9 displays the percentage difference between the individual angular sizes predicted according to the semiempirical narrowband (BL) and empirical broadband (MI) near-infrared photometry for all the ISO standard stars of Class V and III. The diagram clearly indicates two remarkable differential effects.

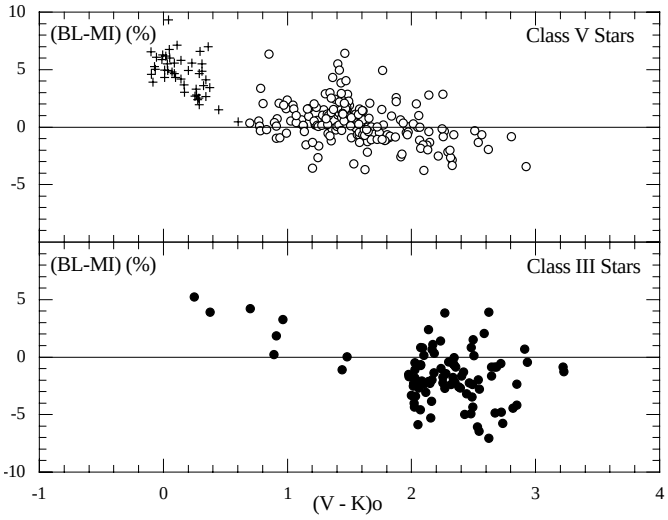

Fig. 9. Comparison between angular diameters predicted by the semiempirical IRFM (BL) and the empirical near-infrared surface brightness technique (MI). Crosses indicate A-type stars

The first most relevant effect is an average systematic difference $(BL-MI) = (4.66 \pm 0.26)$ % over the colour range $-0.1 \leq (V-K)_{\rm O} \leq 0.6$ including the A-type stars. Such an inconsistency has been already stressed in other investigations (Mégessier 1988; Napiwotzki et al. 1993) and can be now revisited. Since it is unlikely that the $(S_{\rm V}, V-K)$ correlation be responsible for the observed deviation, taking into account

Table 6. Comparison between measured and predicted integrated fluxes of A-type stars

Star	V_O	$(V - K)_O$	F_{BOL} ($\times 10^{-9}$ W m^{-2})	$\Delta F_{BOL} / F_{BOL}$ (%)
α CMa			114.3 ± 4.4 [a]	
	- 1.442	- 0.099	112.2	- 1.8
α Lyr			30.4 ± 1.2 [a]	
	0.027	- 0.001	27.5	- 9.5
γ Gem			4.73 ± 0.17 [a]	
	1.903	0.028	4.81	1.7
ε Sgr			5.53 ± 0.22 [a]	
	1.798	0.047	5.26	- 4.9
β Car			6.14 ± 0.22 [a]	
	1.645	0.107	5.89	- 4.1
β Leo			3.61 ± 0.13 [a]	
	2.13	0.14	3.72	3.0
α PsA			8.80 ± 0.31 [a]	
	1.160	0.144	9.07	3.1
α Oph			3.65 ± 0.13 [a]	
	2.068	0.379	3.67	0.5
α Aql			12.17 ± 0.46 [a]	
	0.761	0.520	12.01	- 1.3

[a] From Code et al. (1976)

that the photometric angular diameters are closely matched to the most accurate measurements available from interferometry techniques, I have searched for systematic errors in the semiempirical IRFM. The relevant sources of errors which can affect determinations by the IRFM are related to the bolometric flux measurements including the absolute calibration of the observed magnitudes, to the absolute calibration of the near-infrared reference flux and to the model-atmosphere monochromatic flux. First, there seems to be unlikely that bolometric fluxes be responsible for the observed deviations, taking into account the very consistent results of Table 6. In fact, only a flux discrepancy as large as that of α Lyr would lead to the average shift observed for all A-type stars. Second, a significant error induced by the absolute calibration of the reference flux is also unlikely. Indeed, the comparison of the actual large deviation with the much smaller average value of $(BL - MI) = (0.33 \pm 0.13)$ % derived for dwarfs over the colour range $0.7 \leq (V - K)_{\rm O} \leq 3.0$, would provide the most convincing result that the absolute flux calibration could shift the data by no more than 1 %. Therefore, only the infrared monochromatic fluxes of A-type stars from the new LTE line-blanketed model atmospheres adopted by BL seem to be likely responsible for the observed systematic deviations. In this respect, notice the significant improvement between empirical and semiempirical estimates observed over the F-G-K spectral range.

The second effect is an intrinsic dispersion as large as about $\pm$ 2 % regardless the spectral classification of the stars. By assuming that the bolometric flux measurements and the broadband near-infrared colours be responsible for the observed scatter, it would imply flux errors as large as $\pm$ 4 %, not detected, however, in the $F_{\rm K}$ correlations of Fig. 4. Then, we are compelled again to investigate for random errors arising in the narrowband photometric data and/or the monochromatic model fluxes adopted by the IRFM. A valuable test for assessing the

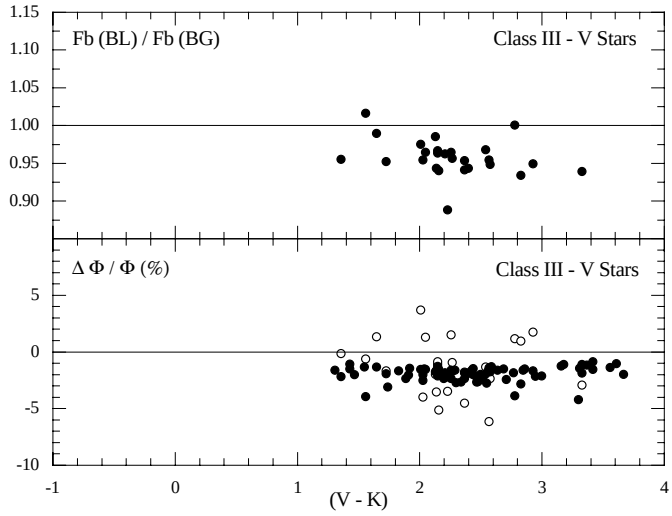

Fig. 10. Comparison between angular diameters predicted by wideband (BG) and narrowband (BL) versions of IRFM and the near-infrared surface brightness technique. Top: normalization of BG to BL bolometric flux measurements. Bottom: wideband (solid circles) and narrowband (open circles) results by IRFM

observed dispersion is drawn in Fig. 10, where angular sizes predicted by two different versions of the IRFM are differentially compared with the actual broadband data. The BG version of the IRFM derives the near-infrared reference flux according to data just using Johnson broadband *K* magnitudes, whereas the BL version for the subset of stars in common is currently adopting specific narrowband filters. For self consistent comparisons, the BG bolometric fluxes should be multiplied by the average correction factor 0.958 derived from the subset of stars in common as reported in the upper part of the diagram. Then, the lower diagram shows the BL data with a dispersion nearly close to those of Fig. 9, as expected. In contrast, the BG data no longer display the high level of scatter as the BL results. Assuming that the LTE line-blanketed and MARCS code model atmospheres adopted by BL and BG, respectively, give rise to consistent results with a small dispersion, according to the BL investigation, there would be evidence for a significantly larger component of random errors arising in the narrowband near-infrared data of the IRFM compared to the version using broadband photometry.

The diagrams of Fig.s 9 and 10 can be readily exploited to assess systematic and random errors affecting the semiempirical narrowband temperatures by the IRFM, since the bolometric fluxes were assumed to be the same in both semiempirical and empirical methods. The significant systematic shift makes the IRFM temperatures of A-type stars too low by 2.33 % (SD = 0.9 %), whereas the average shifts of 0.17 % (SD = 0.9 %) and − 0.93 % (SD = 1.1 %) for dwarfs and giants, respectively, indicate much more consistent results over the F-G-K spectral range. Of course, this fair good agreement between the independent results gives also the most valuable and strong support to the reliability of temperature determinations at the target accuracy of ± 1 % required for the ISO standard stars.

6. The metallicity and gravity effects

One problem of concern is to evaluate gravity and metallicity effects on the stellar parameters derived for field stars. In fact, *at least* for bolometric flux measurements, these effects become now detectable using the high-precision broad-band photometry of the ISO standards. In order to better see the different role played by these effects, I begin to plot the $(B-V, V-K)$ diagram of Fig. 11 for dwarfs and giants separately. In fact, the model-atmosphere calculations of BG make it clear that the gravity and metallicity will have negligible effects on the near-infrared colour adopted here as a practically unbiased temperature indicator. Also, the high-gravity/metal-poor dwarfs will have bluer $(B-V)_{\rm O}$ colours than low-gravity/metal-normal giants with the same temperature (Kurucz 1991), as clearly appear in the actual two-colour diagram. Then, with reference to the residuals of Fig. 4, the smaller scatter observed on the high-gravity/metal-poor dwarfs quite consistent with the random errors on photometry alone indicates that the corresponding bolometric fluxes would be rather insensitive to the widely differing poorer metallicity and practically constant gravity of these stars, whereas the gravity rather than metallicity must be likely responsible for the increased scatter in the flux measurements of low-gravity/metal-normal giants. Also, the small average differential effects drawn in Fig. 5 are likely to be ascribed to gravity which would make the near-infrared colour of giants smaller than that of dwarfs according to the relation (8) and to the model-atmosphere results of BG.

The influence of metallicity on bolometric flux determinations of F-G-K dwarfs has been recently stressed by Alonso et al. (1995) using a sample of stars with most of metallicities measured by high dispersion spectroscopy. For a subset of 49 stars in common with the ISO standards, the effect of the metallicity gradient is clearly observed in the upper plot of Fig. 12 which shows the colour residuals from ridge-line representation drawn in Fig. 11. The middle and lower plots show the bolometric flux residuals from the average third-order polynomial function $F_{\rm BOL}$(AL) and second-order one $F_{\rm BOL}$(MI), respectively. As it can be seen, there is no evidence for any systematic deviation from the actual second-order regression line representing Class V stars, in contrast with the remarkable trend suggested by Alonso et al.. In fact, these authors accounted for the effects of metallicity by using a model-fitting approach rather than to attempt detection of such systematic variations readily observed in the diagram of the metallicity-sensitive colour $(B-V)$. Notice also that the model-dependent flux variations adopted by Alonso et al. would imply temperature shifts by up to 2.5 % at stellar metallicities as poor as − 3.5 dex. Such large systematic effects indeed appear in the final temperature scales derived by the authors (Alonso et al. 1996).

7. Conclusions

The direct method applying the near-infrared surface brightness technique along with bolometric flux measurements has been implemented to determine individual temperatures as accurate as ± 1 % for a sample of 537 A-F-G-K dwarfs and giants

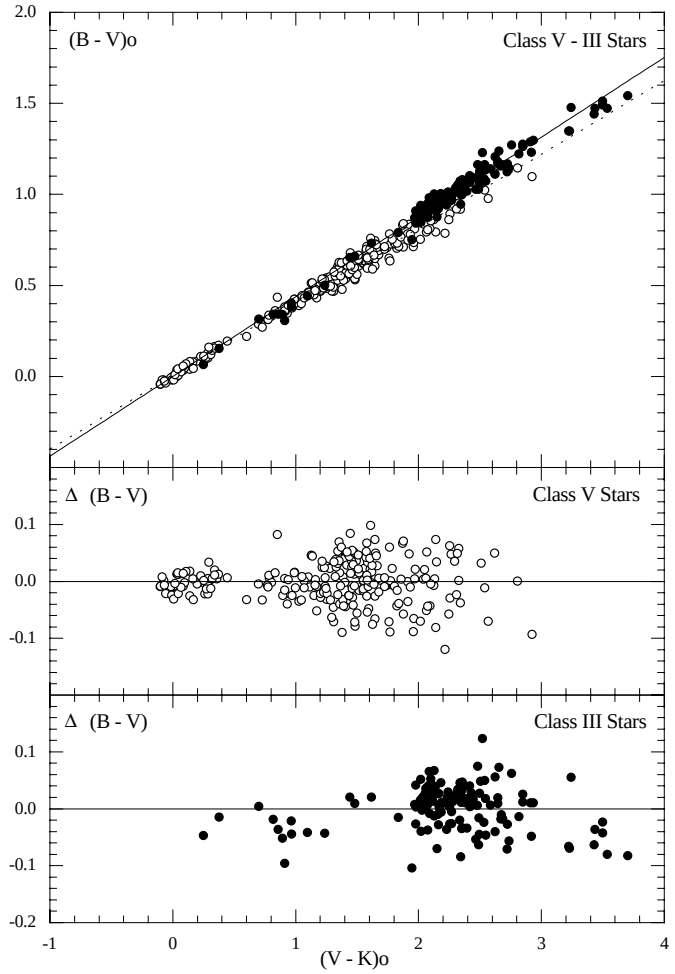

Fig. 11. Metallicity and gravity effects on the optical colour $(B-V)$ of field stars against the intrinsic near-infrared colours. Top: plots of individual data with dotted and solid lines representing linear least-squares fits to Class V and III stars, respectively. Middle and bottom: residuals around the ridge-lines

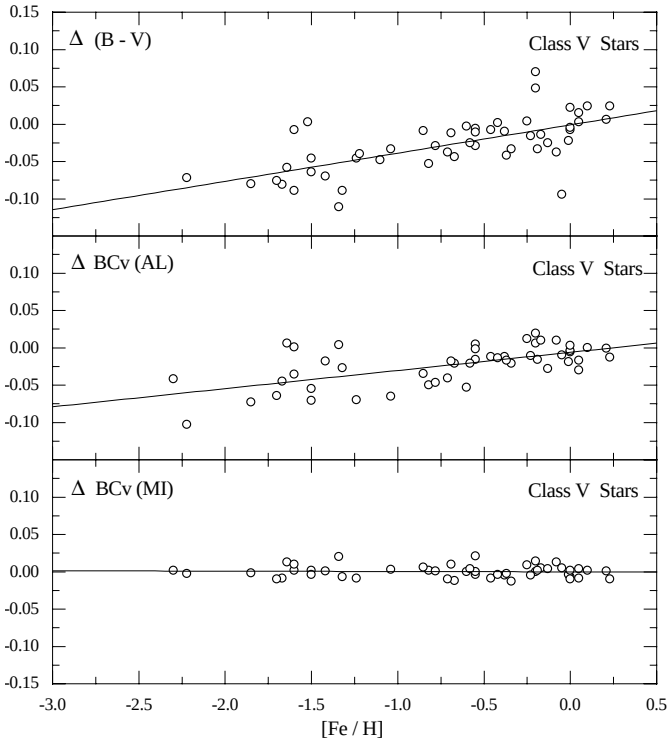

Fig. 12. The effect of metallicity on optical colour and bolometric flux measurements of field dwarfs against the metallicity gradient. Top: colour residuals from the ridge-line drawn in Fig. 11. Middle: flux residuals according to third-order polynomials (see top of Fig. 6). Bottom: flux residuals according to second-order polynomials (see bottom of Fig. 6)

selected as ISO standard stars. The investigation shows that the required target accuracy is within the reach of the carefully calibrated photometric correlations as a function of the Johnson broadband colour $(V-K)$ notably using the high-precision near-infrared *K* magnitudes obtained for this purpose and Hipparcos parallaxes for interstellar reddening corrections. These improvements enable so tight correlations for bolometric flux parameters that gravity effects become now detectable in the field of giants, whereas the much tighter correlations of dwarfs do not show any signature of metallicity up to the intrinsic scatter set by the observational photometry despite the wide range in metal content for these stars.

The small residual coupling with model-atmosphere calculations required to evaluate systematic corrections in measurements of calibrating angular diameters (limb-darkening) and bolometric fluxes (energy in gaps between observed wavelenghts) makes the actual empirical approach as the best available approximation to fundamental stellar parameters over the sampled temperature range. Hence, these data can be exploited as suitable references to assess random and systematic errors affecting semiempirical methods closely related to model-atmosphere predictions as well as to calibrate different photometric relationships.

Acknowledgements. I am indebted to the ISO Ground Based Preparatory Programme Working Group which entrusted me with the actual investigation. It is also a pleasure to thank Drs. N.S. van der Bliek, J. Manfroid, P. Bouchet and P. L. Hammersley who kindly provided me with the observational photometry in advance of publication. Hipparcos parallaxes were provided by Dr. M. Perryman also in advance of publication. I am especially grateful to Prof. D. E. Blackwell who kindly made the bolometric flux determinations available to me in advance of publication.

References

Alonso A., Arribas S., Martinez-Roger C., 1995, A&A 297, 197
Alonso A., Arribas S., Martinez-Roger C., 1996, A&A 313, 873
Barnes T.G., Evans D.S., Moffett T.J., 1978, MNRAS 183, 285
Bell R.A., Gustafsson B., 1989, MNRAS 236, 653
Blackwell D.E., Lynas-Gray A.E., 1998, A&A in press
Blackwell D.E., Petford A.D., Arribas S., Haddock D.J., Selby M.J., 1990, A&A 232, 396
Campins H., Rieke G.H., Lebofsky M.J., 1985, AJ 90, 896
Code A.D., Davis J., Bless R.C., Hanbury Brown R., 1976, ApJ 203, 417

Cohen M., Walker R.G., Barlow M.J., Deacon J.R., 1992, AJ 104, 1650
Davis J., Tango W.J., 1986, Nat 323, 234
Di Benedetto G.P., 1993, A&A 270, 315
Di Benedetto G.P., Bonneau D., 1991, A&A 252, 645
Di Benedetto G.P., Rabbia Y., 1987, A&A 188, 114
ESA, 1997, The Hipparcos Catalogue ESA SP-1200
Forgan B.W., 1977, Appl. Optics 16, 1628
Hummel C.A., Armstrong J.T., Quirrenbach A., et al., 1994, AJ 107, 1859
Hutter D.J., Johnston K.J., Mozurkewich D., et al., 1989, ApJ 340, 1103
Kurucz R.L., 1991, Stellar Atmospheres: Beyond Classical Models, NATO ASI Series, vol. 341, ed. L. Crivellari, I. Hubeny, D.G. Hummer, p. 441
Manduca A., 1979, A&AS 36, 411
Mégessier C., 1988, A&AS 72, 551
Mozurkewich D., Johnston K.J., Simon R.S., et al., 1991, AJ 101, 2207
Napiwotzki R., Schonberner D., Wenske V., 1993, A&A 268, 653
Quirrenbach A., Mozurkewich D., Buscher D.F., Hummel C.A., Armstrong J.T., 1996, A&A 312, 160
Ridgway S.T., Joyce R.R., White N.M., Wing R.F., 1980, ApJ 235, 126
Ridgway S.T., Jacoby G.H., Joyce R.R., Siegel M.J., Wells D.C., 1982, AJ 87, 1044
van der Bliek N.S., Bouchet P., Habing H.J., et al., 1992, ESO Messenger 70, 28
van der Bliek N.S., Manfroid J., Bouchet P., 1996, A&AS 119, 547
Turon C., Egret D., Gomez A., et al., 1992, The Hipparcos Input Catalogue ESA SP-1136
Wegner W., 1994, MNRAS 270, 229
Wesselink A.J., 1969, MNRAS 144, 297